Electromechanical grain boundary model with formation mechanism in polycrystalline ferroelectrics ⊘

Xuhui Lou ; Xu Hou ; Yujun Chen; Jianxiang Wang ; Shengyou Yang ; Haidong Fan ;
Jie Wang ✉ ; Xiaobao Tian ✉

Check for updates

View Online   Export Citation

Articles You May Be Interested In

Ferroelectric domain switching pathways—From grain boundary to grain body

Appl. Phys. Lett. (May 2023)

From the flow to the polarization field: A cognitive way for ferroelectric vortex structures

Appl. Phys. Lett. (June 2022)

Observation of high dielectric constants in x (Pb (Zn 1∕3 Nb 2∕3) O 3 – (0.2 − x) Pb (Ni 1∕3 Nb 2∕3) O 3 – 0.8 Pb (Zr 1∕2 Ti 1∕2) O 3 ternary solid solutions

J. Appl. Phys. (November 2007)

06 January 2025 07:46:18

Electromechanical grain boundary model with formation mechanism in polycrystalline ferroelectrics

Xuhui Lou,[1,2] Xu Hou,[3,4] Yujun Chen,[1,2] Jianxiang Wang,[5,6] Shengyou Yang,[7] Haidong Fan,[2] Jie Wang,[3,8,a)] and Xiaobao Tian[1,2,a)]

AFFILIATIONS

[1]MoE Key Laboratory of Deep Earth Science and Engineering, College of Architecture and Environment, Sichuan University, Chengdu 610065, People's Republic of China
[2]Department of Mechanics and Engineering, Sichuan University, Chengdu, Sichuan 610065, People's Republic of China
[3]Department of Engineering Mechanics and Key Laboratory of Soft Machines and Smart Devices, College of Aeronautics and Astronautics, Zhejiang University, Hangzhou 310027, People's Republic of China
[4]Department of Industrial and Systems Engineering, The Hong Kong Polytechnic University, Hung Hom, Kowloon, Hong Kong, China
[5]State Key Laboratory for Turbulence and Complex Systems, Department of Mechanics and Engineering Science, College of Engineering, Peking University, Beijing 100871, People's Republic of China
[6]CAPT-HEDPS, and IFSA Collaborative Innovation Center of MoE, Peking University, Beijing 100871, People's Republic of China
[7]School of Civil Engineering, Shandong University, Jinan, 250061, People's Republic of China
[8]Zhejiang Laboratory, Hangzhou, Zhejiang 311100, China

[a)]**Authors to whom correspondence should be addressed:** jw@zju.edu.cn and xbtian@scu.edu.cn

ABSTRACT

Grain boundaries (GBs) are transitional, defective, and anisotropic interfaces between adjacent grains with different orientations. However, most models assume that the GB is an isotropic dielectric determined by itself and lacks formation information; these assumptions hinder the theoretical investigation of the effect GBs have on polycrystalline ferroelectrics at the mesoscopic scale. Here, a novel GB model based on the formation mechanism is established for ferroelectric polycrystals. It has been found that the Curie–Weiss temperature range, elastic coefficient, and permittivity of GBs are related to the orientation of adjacent grains and the polarization state. The shielding effect, polarization enhancement, domain continuity, and spontaneous polarization on the GBs are obtained in mesoscopic simulations based on this model. In addition, the proportion of GBs can significantly affect the electric field distribution in grains. It provides a mechanistic explanation for the relationship between the coercive electric field and the proportion of GBs in the previous experiment. By achieving a better mesoscopic description of GBs, the GB model proposed in this work provides an effective investigation tool for electromechanical, electrocaloric, and energy storage of polycrystalline functional materials.

Published under an exclusive license by AIP Publishing. https://doi.org/10.1063/5.0120308

I. INTRODUCTION

Ferroelectric ceramics are widely used in microelectronic devices because of their excellent dielectric and electromechanical properties.[1] Most ferroelectric ceramics are polycrystalline, composed of grains with different orientations and structures and grain boundaries (GBs), which are observed to exist in different domain distributions when studied using dark field x ray.[2,3] A polarization domain is a collection of long-range elastic and short-range electrostatic interactions in all grains and GBs.[4] A GB presents as a weak ferroelectric region with defects and dislocation aggregation.[5,6] The

microstructure of a GB has an important influence on the continuous distribution of domains between adjacent grains.[7,8] Additionally, because of the anisotropy of ferroelectric crystals, the grain orientation affects the domain distribution and the reformation of the GB structure.[9,10] Designing the GB to control domains attracts increasing attention in interface engineering, and understanding the effects of the GB on domain structure and switching in ferroelectric ceramics becomes a fundamental issue.

For polycrystalline ferroelectric ceramics, many theoretical studies have been carried out to investigate the GB. Based on the thermodynamics method, Choudhury *et al.* proposed a three-dimensional phase field interface model with periodic boundary conditions and simulated the influence of the GB on the formation and growth of domain structure, finding that domain switching generally occurs near the GB.[11,12] This no-thickness interface model simplifies the details of GBs and focuses on the effect of the shape and orientation of grains on the distribution of domains. By considering the GB as an amorphous weak dielectric with isotropic properties, Frey *et al.* proposed the "dead layer" interphase model in 1998.[13] Based on this model, the effects of grain size, GB thickness, and dielectric constant on the overall ferroelectricity and dielectric properties of barium titanate ceramics have been measured.[14] GB size can affect the domain evolution of polycrystalline ferroelectrics.[4,15] The "dead layer" interphase model emphasizes the GB structural disorder, strengthens the depolarization effect of the GB on grains, and weakens the domain continuity between grains. A new GB model was recently proposed from the perspective of core–shell composite materials. This core–shell model did not consider the effect of the orientation of adjacent grains in polycrystalline ferroelectrics.[16] Both classic models agree well with the experimental results when the proportion of GBs is small. However, with the miniaturization of ceramic electronic components, the influence of GBs becomes more significant as their proportion increases or the grain size decreases. Establishing a new GB model based on the formation mechanism is highly expected to solve the shortcomings mentioned above.

At the atomic scale, the $\Sigma 5$ (001) twin boundary energy between twin crystals with a misorientation of $36.9°$ exhibits spontaneous linear polarization and vortex polarization in the GB.[17] Furthermore, the GB can maintain the continuous distribution of domains in polycrystalline ferroelectrics and induce anti-vortex domains.[18] These results indicate that the GB plays an important role in the regulation and utilization of polarization domains; therefore, establishing a comprehensive GB model based on the formation mechanism will broaden the application of interface engineering.[19,20] It is well known that the GB is a three-dimensional interface defect formed by the combination of two grains with different orientations. Considering the important influence of grain orientation on the structure of GBs, there is a need to establish a model for an accurate description of domain evolution.

A theoretical model based on the formation mechanism of GB (FMGB) is proposed in Sec. II. A GB is a transition region formed by the orientation difference between adjacent grains.[21] The macroscopic material parameters of GBs largely depend on the orientation difference. Section III provides an analysis of the influence of grain orientation difference on the GB parameters such as the Curie–Weiss temperature, elastic coefficient

characteristic coefficient, and permittivity. Section IV compares the new model with the previous models in BaTiO$_3$ twin crystals to investigate its reliability.

II. GB FORMATION MECHANISM MODEL

GBs in ferroelectric polycrystals have attracted tremendous interest owing to their properties, such as dislocations, GB orientation,[6] twisted GBs,[22] and GB space charge.[23,24] It has been found that the GB has a larger local elastic energy and stronger shielding effect than the bulk grain, which hinders the polarization domain movement crossing GBs. However, the structures of a GB, such as space charge and porosity, are limited by experimental conditions and cannot be measured and analyzed directly, making it difficult to accurately describe the effects of grains and GBs on the domain structure.[25–28]

Based on the GB formation mechanism, polycrystalline ferroelectrics are composed of grains and GBs, as shown in Fig. 1(a). Therefore, the total bulk energy density of polycrystalline f_{poly} from thermodynamics theory can be expressed as

$$f_{poly} = \sum f_{grain} + \sum f_{gb}, \tag{1}$$

where f_{grain} and f_{gb}, respectively, represent the energy density of individual grains and GBs. It includes the free-energy density f_{bulk}, elastic energy density f_{elas}, coupling energy density f_{coup}, gradient energy density f_{grad}, and electric energy density f_{elec} and can be expressed as

$$f_{grain/gb} = f_{bulk} + f_{elas} + f_{coup} + f_{grad} + f_{elec}. \tag{2}$$

The free-energy density f_{bulk} is related to the Curie–Weiss temperature $T_{g/gb}$ of ferroelectrics, as $f_{bulk}(T_{g/gb})$. Although the Curie–Weiss temperature T_g is a constant in grains, the $T_{gb(m-n)}$ at GBs is related to the orientation difference of adjacent grains $\Delta\theta_{(m-n)}$.[17] It should be noted that only the symmetric tilt GBs be considered in this work to simplify the analyzation. Based on the symmetric tilt GBs assumption, the related properties of GBs can be described only by $\Delta\theta_{(m-n)}$. Here, $\theta_{gb(m-n)}$, θ_m, and θ_n, respectively, represent the orientation of the GB, the adjacent grain m and grain n and can be expressed as follows:

$$\Delta\theta_{(m-n)} = |\theta_m - \theta_n|, \tag{3}$$

$$\theta_{gb(m-n)} = \min\{\theta_m, \theta_n\} + \frac{1}{2}\Delta\theta_{(m-n)}. \tag{4}$$

Therefore, the f_{bulk} at GBs can be expressed as a function of the orientation, $f_{bulk}(\theta_{gb(m-n)})$. The elastic energy density f_{elas} is related to the elastic coefficient. For grains, the elastic coefficient $\mathbf{c}_g$ is a constant, and for GBs, $\mathbf{c}_{gb(m-n)}$ is related to $\Delta\theta_{(m-n)}$, $f_{elas}(\theta_{gb(m-n)})$.[29] Similar to $\mathbf{c}_{gb(m-n)}$, the permittivity $\kappa_{gb(m-n)}$ of GBs is related to $\Delta\theta_{(m-n)}$,[30] which affects the electric energy density $f_{elec}(\theta_{gb(m-n)})$. The coefficients of f_{coup} and f_{grad} are assumed to be constant for both grains and GBs.
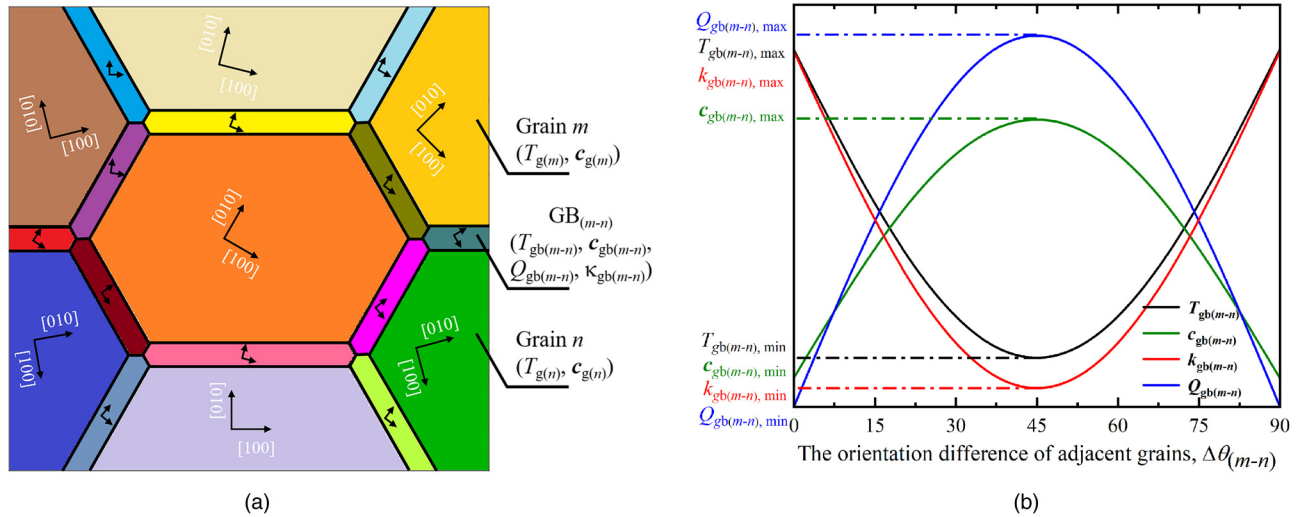
FIG. 1. Polycrystalline model and the FMGB model. (a) Polycrystalline ferroelectrics, GB orientation, and parameters are affected by adjacent grain *m* and grain *n*. (b) Variation of GB parameters with misorientation of the adjacent grains.

Based on the previously described analysis and the formation mechanism of the GB, a new FMGB model is established in this work as

$$
\begin{cases}
f_{gb}(T_{gb(m-n)}, c_{gb(m-n)}, \kappa_{gb(m-n)}) \\
\quad = f_{bulk}(T_{gb(m-n)}) + f_{elas+coup}(c_{gb(m-n)}) + f_{grad} + f_{elec}(\kappa_{gb(m-n)}), \\
T_{gb(m-n)} = (1 - \mu_T \sin(2\Delta\theta_{(m-n)}))T_g, \\
c_{gb(m-n)} = (1 + \mu_c \sin(2\Delta\theta_{(m-n)}))c_g, \\
\kappa_{gb(m-n)} = (1 - \mu_\kappa \sin(2\Delta\theta_{(m-n)}))\kappa_g, \\
Q_{gb(m-n)} = Q\sin(2\Delta\theta_{(m-n)}),
\end{cases} \quad (5)
$$

where κ_g represents the permittivity of grains, $Q_{gb(m-n)}$ is the space-charge density on the GB, and Q is the maximum density of space-charge. μ_T, μ_c, and μ_κ, respectively, represent the characteristic coefficients of the Curie–Weiss temperature, elastic coefficient, and permittivity. Considering a cubic crystal grain with a symmetrical structure, the sinusoidal periodic function is introduced to describe the relationship between material parameters of [001] GBs and misorientation, while the misorientation of adjacent grains $\Delta\theta_{(m-n)}$ is between 0° and 45°. For other types of GBs, the maximum misorientation will be different as crystal symmetry, for example, the maximum misorientation of [111] GBs is 30°. The sinusoidal function is also used in the Read–Shockley model to describe the dislocation density,[31,32] especially for the symmetric tilt GBs. $\Delta\theta_{(m-n)} = 0°$ means that the grain orientations on either side of the GB are the same; thus, the parameters of the GB are consistent with that of grains. $\Delta\theta_{(m-n)} = 45°$ means that the grain orientation difference on both sides of the GB is at its maximum, and the aggregation density of defects and dislocations on the GB also reaches its maximum, as shown in Fig. 1(b). The coefficient $\mu_i (i = T, c, \kappa)$ characterizes the degree of grain orientation difference on the GB.

This formation mechanism model can characterize the electromechanical properties of grain boundaries as those of the general grain. However, based on Ginzburg–Landau thermodynamic theory for ferroelectrics,[33] the energy density f_{grain} of grains can be expressed as a function of local polarization P_k^L, polarization gradient $P_{k,l}^L$, strain ε_{kl}^L, and electric field E_k^L, where $k, l = 1, 2, 3$. By analogy with f_{grain}, f_{gb} can also be expressed as a function of P_k^L, $P_{k,l}^L$, ε_{kl}^L, and E_k^L for individual GBs. The superscript L indicates the local coordinate, and the energy density f_{grain} of the grain can be simplified by setting $\Delta\theta_{(m-n)} = 0°$ for the GB-related parameters. f_{gb} can be given as

$$
f_{gb}(P_k^L, P_{k,l}^L, \varepsilon_{kl}^L, E_k^L) = f_{bulk}(P_k^L) + f_{elas}(\varepsilon_{kl}^L) + f_{coup}(P_k^L, \varepsilon_{kl}^L) \\
+ f_{grad}(P_{k,l}^L) + f_{elec}(P_k^L, E_k^L). \quad (6)
$$

The free-energy density $f_{bulk}(P_k^L)$ of the GB is usually expanded as the higher-order polynomial of a spontaneous polarization, which can be expressed as

$$
f_{bu1ptlk}(P_k^L) = \alpha_{kl}P_k^L P_l^L + \alpha_{klop}P_k^L P_l^L P_o^L P_p^L \\
+ \alpha_{klopqr}P_k^L P_l^L P_o^L P_p^L P_q^L P_r^L, \quad (7)
$$

where α_{klop} and α_{klopqr} are the higher-order dielectric constants. α_{kl} is the GB dielectric coefficient related to GB Curie–Weiss temperature, as shown in Eq. (5), which can be expressed as

$$
\alpha_{kl} = \frac{T - T_{gb(m-n)}}{2\kappa_0 C_0} = \frac{T - T_g + T_g \cdot \mu_T \sin(2\Delta\theta_{(m-n)})}{2\kappa_0 C_0}, \quad (8)
$$

where T is the ambient temperature, κ_0 is the vacuum dielectric coefficient, and C_0 is the Curie constant. Therefore, $f_{bulk}(T_{gb(m-n)})$ can be described by $f_{bulk}(P_k^L)$ based on Eq. (8).

The strain and coupling energy density can be expressed as

$$f_{e1ptla1pts}(\varepsilon_{kl}^L) + f_{coup}(P_k^L, \varepsilon_{kl}^L) = \frac{1}{2}\mathbf{c}_{klop}\varepsilon_{kl}^L\varepsilon_{op}^L$$
$$- q_{klop}\varepsilon_{kl}^L P_o^L P_p^L + r_{klopqr}\varepsilon_{kl}^L\varepsilon_{op}^L P_q^L P_r^L$$
$$+ s_{klopqr}\varepsilon_{kl}^L P_o^L P_p^L P_q^L P_r^L,$$

$$(9)$$

where c_{klop} indicates the GB elasticity coefficient, as shown in Eq. (5). Therefore, $f_{elas+coup}(c_{gb(m-n)})$ can be described by $f_{elas}(\varepsilon_{kl}^L)$ $+f_{coup}(P_k^L, \varepsilon_{kl}^L)$, q_{klop}, r_{klopqr}, and s_{klopqr}, which are the electrostrictive coefficients.

Because of the complexity of domains within the GB, the gradient energy formed by the discontinuity of polarization between domains is non-negligible, which can be expressed as

$$f_{grad} = g_{klop}P_{k,l}^L P_{o,p}^L,$$

$$(10)$$

where g_{klop} is the gradient coefficient of GBs, which is consistent with that of the grains.

When an electric field E_k^L is applied to polycrystals, the electric field energy density can be expressed as

$$f_{e1ptle1ptc}(P_k^L, E_k^L) = -\frac{1}{2}\kappa_{gb}E_k^L E_k^L - E_k^L P_k^L,$$

$$(11)$$

where κ_{gb} is the permittivity of GBs as shown in Eq. (5) and $f_{elec}(\kappa_{gb(m-n)})$ can be described by $f_{elec}(P_k^L, E_k^L)$.

Compared with grains, the main difference is that the energy density at the GB is related to the orientation difference $\Delta\theta_{(m-n)}$ between adjacent grains and its own orientation $\theta_{gb(m-n)}$. When calculating the GB energy, it is necessary to use the coordinate conversion equation to convert the local coordinate into a global coordinate. The orientation of GB can be represented by a set of Euler angles (α, β, θ).[11] The variables P_k^L, E_k^L, and ε_{kl}^L can be converted from local to global coordinates using the formula $\vec{\mathbf{P}}^L = \bar{\mathbf{R}}\vec{\mathbf{P}}$, $\vec{\mathbf{E}}^L = \bar{\mathbf{R}}\vec{\mathbf{E}}$, $\hat{\boldsymbol{\varepsilon}}^L = \bar{\mathbf{R}}^T\hat{\boldsymbol{\varepsilon}}\bar{\mathbf{R}}$, where $\bar{\mathbf{R}}$ is a conversion matrix. This study only considered GBs in a two-dimensional plane and rotated along the x_3-axis, that is, the [001] direction; therefore, the matrix can be expressed as

$$\bar{\mathbf{R}} = \begin{pmatrix} \cos\theta_{gb(m-n)} & \sin\theta_{gb(m-n)} & 0 \\ -\sin\theta_{gb(m-n)} & \cos\theta_{gb(m-n)} & 0 \\ 0 & 0 & 1 \end{pmatrix}.$$

$$(12)$$

The evolution of spatially inhomogeneous polarization can be obtained from the time-dependent Ginzburg–Landau (TDGL) as[34]

$$\frac{\partial P_i(\mathbf{r}, t)}{\partial t} = -L\frac{\delta f}{\delta P_k(\mathbf{r}, t)} \quad (i = 1, 2),$$

$$(13)$$

where t denotes the time, L is the kinetic coefficient of domain switching, $\delta f/\delta P_k(r, t)$ denotes the thermodynamic drivers of polarization evolution, and r is the spatial vector, $r = (x_1, x_2)$.

For body-charge-free and body-force-free polycrystalline ferroelectrics, the mechanical equilibrium $\partial(\partial f/\partial\varepsilon_{kl})/\partial x_l = 0$ and Maxwell equilibrium $\partial(-\partial f/\partial E_k)/\partial x_k = 0$ should also be satisfied.

III. MODELING THE ELECTROMECHANICAL CHARACTERISTIC COEFFICIENTS OF GB

A. GB Curie–Weiss temperature characteristic coefficient

The Curie–Weiss temperature characteristic coefficient μ_T of the GB strongly correlates with its own state, and the analysis of the value range of μ_T plays a crucial role in investigating the ferroelectricity of the GBs. The range of μ_T is the first step for model application. Equation (S1) in the supplementary material considers the energy density function f_{μ_T} of the GB without an external field, including free-energy density in global coordinates. It analyzes the minimum value $\partial f/\partial P_k = 0$ and derives the value of the second-order partial derivative $\partial^2 f/\partial P_k^2$.

In ferroelectrics, the energy minimum always occurs in the direction of the crystallographic axis.[8] Therefore, the spontaneous polarizations P_1 and P_2 should follow that rule such that

$$P_2 = P_1\tan(\theta_{gb(m-n)}).$$

$$(14)$$

Substituting Eq. (14) into the second-order partial derivative $\partial^2 f/\partial P_k^2$ from Eq. (S1) in the supplementary material gives

$$\frac{\partial^2 f}{\partial P_1^2} = \frac{2\alpha_{gb(m-n)}}{\cos^2(\theta_{gb(m-n)})} + \frac{12\alpha_{11}}{\cos^4(\theta_{gb(m-n)})}P_1^2 + \frac{30\alpha_{111}}{\cos^6(\theta_{gb(m-n)})}P_1^4. \quad (15)$$

The GB is in a paraelectric state if $P_1 = 0$ and $T_g > T > T_{gb(m-n)}$, which means Eq. (15) should be greater than zero.[1] Then, the range of μ_T can be derived as

$$\mu_T > \frac{T_g - T}{T_g\sin(2\Delta\theta_{(m-n)})}.$$

$$(16)$$

The GB is in a ferroelectric state if $T < T_{gb(m-n)} < T_g$, which means Eq. (15) should be less than zero. μ_T can be derived as

$$0 < \mu_T < \frac{T_g - T}{T_g\sin(2\Delta\theta_{(m-n)})}.$$

$$(17)$$

Based on Eqs. (16) and (17), the value range of the Curie–Weiss temperature characteristic coefficient μ_T is shown in Fig. 2. When the GB is in a paraelectric state (red area), there is a theoretical lower limit for the characteristic coefficient μ_T, which is related to the adjacent grain orientation difference $\Delta\theta_{(m-n)}$, but no upper limit exists. When $\mu_T \to +\infty$, the GB can be considered to be in an amorphous state without spontaneous polarization, which is consistent with the "dead layer" interphase assumption. When the GB is in a ferroelectric state (blue area), there is a theoretical upper limit for the characteristic coefficient μ_T. This implies that when the characteristic coefficient is lower than this value, the GB theoretically has spontaneous polarization, which has been mentioned elsewhere in the literature.[17]
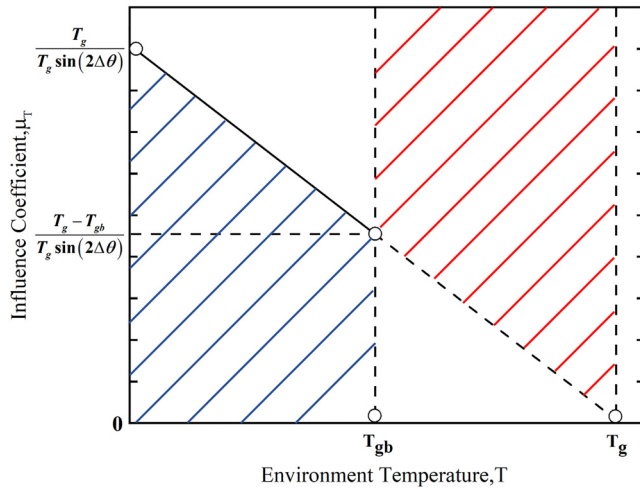
FIG. 2. Value range of the Curie–Weiss temperature characteristic coefficient μ_T. Blue lines indicate that the GB is in a ferroelectric state, and red lines indicate that the GB is in a paraelectric state.

B. GB elasticity characteristic coefficient

To analyze the value range of the GB elasticity characteristic coefficient μ_c, the energy density function f_{μ_c}, Eq. (S3) in the supplementary material, including free-energy density, elastic, and coupling energy density in the global coordinate, can be analyzed.

Based on the mechanical equilibrium equation $\partial(\partial f/\partial\varepsilon_{kl})/\partial x_l = 0$, the GB elastic coefficient $c_{gb(m-n)}$ is assumed to be a position-independent parameter. The elastic characteristic coefficient μ_c can be expressed as

$$\mu_c = \frac{q_{11}\lambda_1 + q_{12}\lambda_2 + 2q_{44}\lambda_3}{(c_{11}\zeta_1 + c_{12}\zeta_2 + 4c_{44}\zeta_3)\sin(2\Delta\theta_{(m-n)})} - \frac{1}{\sin(2\Delta\theta_{(m-n)})}, \tag{18}$$

where the definitions of ζ_1, ζ_2, ζ_3, λ_1, λ_2, λ_3 related to polarization and strain can be found in Eq. (S5) in the supplementary material. The elastic characteristic coefficient μ_c of the GB is determined by its orientation $\theta_{gb(m-n)}$, misorientation $\Delta\theta_{(m-n)}$, equilibrium polarization, gradient polarization, and the strain and gradient strain of the GB.

C. Permittivity characteristic coefficient of the GB

The GB permittivity characteristic coefficient, μ_κ, is an important mechanic coefficient for the electromechanical coupling performance of GBs. When the electric field E_1 is aligned along the x_1-direction, the total energy density function of the GB $f_{\kappa_{gb}}$ including free-energy density and electric energy density in the global coordinate is expressed by Eq. (S7) in the supplementary material.

When the electric field is large enough, the polarization perpendicular to the electric field direction can be ignored, that is, $P_2 = 0$,

Eq. (S8) in the supplementary material. The equilibrium state of this system can be found by minimizing the equation $\partial f/\partial P_1$, Eq. (S9) in the supplementary material. Taking the partial derivative of Eq. (S9) in the supplementary material, the reciprocal of permittivity can be expressed as Eq. (S10) in the supplementary material.

The spontaneous polarization can be expressed as $P_1 = 0$, if the GB is in a paraelectric state. Then, the GB permittivity characteristic coefficient μ_κ can be obtained as

$$\mu_\kappa = \frac{1}{\sin(2\Delta\theta_{(m-n)})} - \frac{1}{2\alpha_{gb(m-n)}\kappa_0\kappa_g\sin(2\Delta\theta_{(m-n)})}, \tag{19}$$

When the GB is in a ferroelectric state, μ_κ can be expressed as

$$\mu_\kappa = \frac{1}{\sin(2\Delta\theta_{(m-n)})}$$
$$- \frac{1}{(2\alpha_{gb} + 12\xi_1 P_1^2 + 30\xi_2 P_1^4)\kappa_0\kappa_g\sin(2\Delta\theta_{(m-n)})}, \tag{20}$$

where ξ_1, ξ_2 related to higher-order dielectric constants can be expressed as in Eq. (S11) in the supplementary material.

From the above results, when the GB is in a paraelectric state, κ_{gb} is only related to $\alpha_{gb(m-n)}$, Eq. (8). When the GB is in a ferroelectric state, κ_{gb} is not only related to the factors above, but also to the polarization in an equilibrium state.

IV. ELECTROMECHANICAL GB MODEL FOR BI-CRYSTAL NANOSTRUCTURE

In this section, the FMGB model is employed to investigate the weak ferroelectric and size effects of GBs on BaTiO$_3$ bi-crystal samples. The grain size in all modeled samples is 49×98 nm. The width of GB was set as 4.9, 2.45, 1.63, 1.2, and 1 nm in different samples. The width of GB in this paper contains two parts: the width of GB itself and that of the GB affected zone, where the thickness of GB is about 0.8–1.25 nm, and the thickness of the affected zone on one side is about 0.1–0.6 nm. Furthermore, to amplify the effect of GB, an extreme case is adopted so that the thickness of the affected zone on one side is 1.825 nm. The material parameters are given in the supplementary material. At the grain/GB interface, a perfect bonding without stress assumption is adopted.[35] The orientation of grain **1** is 0° and grain **2** is 45°. In Sec. IV A, the proportion of GB is set to 1.2%and the orientation of the GB to $\theta_{gb} = 22.5°$.

The phase field finite element model is shown in Fig. 3(a); an electric field E is applied to the surface along the x_1-direction from the left to the right boundary. The finite element model contains 9801 nodes and 9604 elements, and all elements are 1 nm in size (two lattice sizes), as shown in Fig. 3(b). The Curie–Weiss temperature characteristic coefficient, characteristic elastic coefficient, and permittivity of the FMGB model adopt the results in Sec. III; the spatially accumulated charge on the GB adopts the assumption of Eq. (5). The accumulated space-charge density near GB should be less than the spontaneous polarization of grains and is related to the orientation of the adjacent grains.[36] In this work, the space-charge is assumed to be uniformly distributed in the GB zone, including the positive and negative charges, that is, the total space-charge is
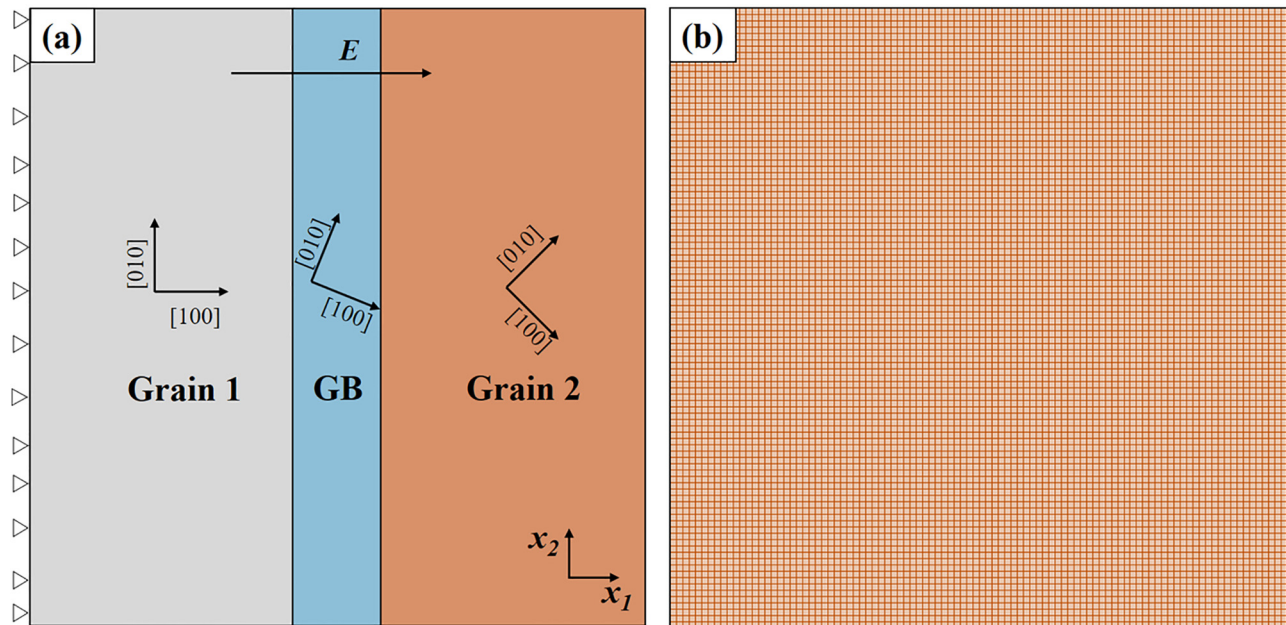
FIG. 3. (a) Phase field modeling of a bi-crystal with an electric field applied along the x_1-direction. (b) A quadrilateral element is used, and the size is 1 nm.

zero. Here, the density of the space-charge is assumed to be $Q = 0.078$ C/m^2, and the distribution of the space-charge is quantitatively consistent with the result of the domain continuity theory,[8] where the charge of $\Delta\theta = 0°$ and $\Delta\theta = 90°$ is zero. In Sec. IV B, by changing the proportion of GB (1%–4.8%), the size effect of the GB in different models is analyzed.

A. Domain structure evolution of GB in an electric field

The evolution of BaTiO$_3$ bi-crystal domains is shown in Figs. 4(a)–4(d). When the electric field is zero [point a in Fig. 4(e)], grain **1** is almost a single domain, and a classical pattern domain structure appears in grain **2**, shown in Fig. 4(a). The polarization inside the GB is weakened but that near the GB is enhanced; this domain phenomenon is consistent with the results obtained by atomic simulations, which report that the biggest or smallest value of polarization is at the grain boundaries.[18] When the electric field increases in the negative direction, the domains gradually flip, and the coercive electric field is considerably strengthened compared with the no-thickness interface model, Fig. S3.1 in the supplementary material. Under the influence of the maximum negative electric field [point b in Fig. 4(e)], because of the mass transfer at the GB and the size of GB being small, almost all domains are aligned in the direction of the electric field, as shown in Fig. 4(b). When the electric field is increased to zero [point c in Fig. 4(e)], the domain structure in Fig. 4(c) is similar to Fig. 4(a), except the direction is changed and retains good polarization properties compared with the "dead layer" interface model, Fig. S3.2 in the supplementary material. At the maximum positive electric field [point d in Fig. 4(e)], the domain structure is similar to Fig. 4(b),

as shown in Fig. 4(d). The relationship between domain state and misorientation is shown in Fig. S3.3 in the supplementary material, and with increasing misorientation, remanent polarization and coercive electric decrease.

Compared with the previous GB models, this FMGB model describes well the weak ferroelectricity of the GB, the polarization enhancement effect at the interface, the shielding effect of the GB in the domain flipping, and the depolarization effect of the GB on adjacent grains. It indicates that this FMGB model not only includes the advantages of the no-thickness interface and "dead layer" interphase GB models but also can simulate some new phenomena of GB. A detailed quantitative comparison of a strain-field loop and a P–E loop with the experimental results[37,38] and molecular dynamics simulation[39] can be found in the supplementary material, and the simulation results are consistent with the experiments.

B. Size effect of GBs in nano ferroelectrics

As the grain size increases in a polycrystalline material, the proportion of GBs decreases correspondingly. Figure 5 shows the polarization vs hysteresis loop lines (P–E loops) at different GB proportions, based on the "dead layer" interphase assumption and the FMGB model. As the GB proportion increases from 1% to 4.8%, the P–E loop of the "dead layer" interphase assumption goes from narrow to wide. When the GB proportion is 1%, the saturation polarization is 175% larger than when the proportion is 4.8%, and the remanent polarization is also 1744% larger. In contrast to the increase in saturation polarization and remanent polarization, the coercive field is almost unchanged. It should be noticed that the ferroelectricity of the bi-crystal disappears based on the P-E
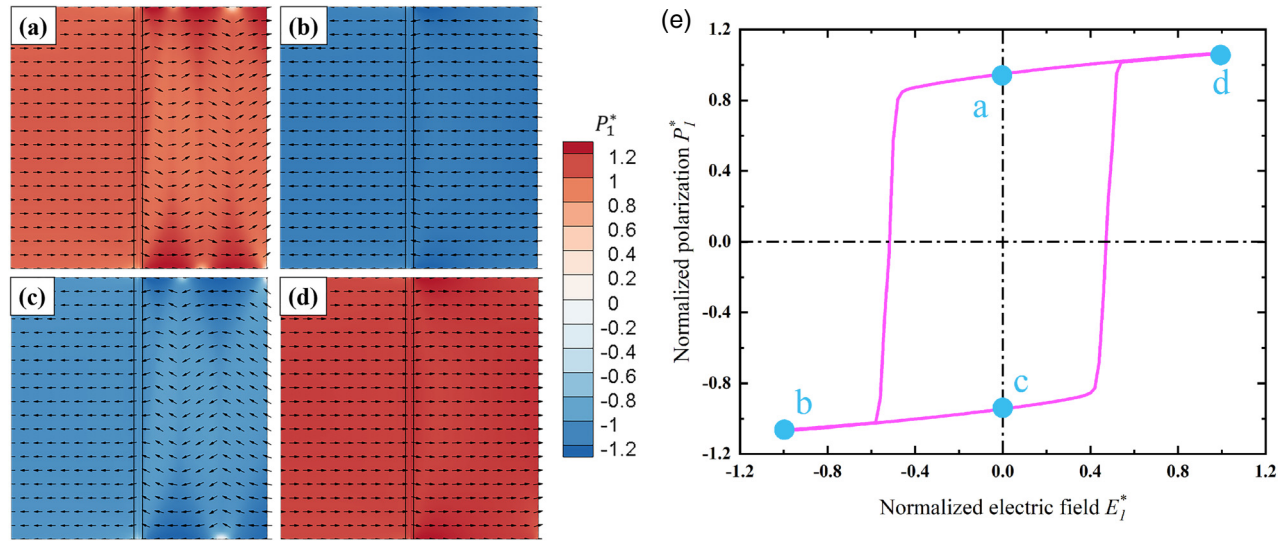
FIG. 4. Domain structure evolution in a BaTiO$_3$ bi-crystal using the FMGB model. (a)–(d) correspond to the four polarization states in (e) (points a–d). The proportion of GB is 4.8%. (e) P–E hysteresis loop of BaTiO$_3$ bi-crystal. Arrows represent polarization vectors, and the background color indicates the distribution of absolute polarization values. $E_1^* = E/E_0$ ($E_0 = 96.5$ kV/cm), $P_1^* = P/P_0$ ($P_0 = 2592$ C/cm^2).

loop when the GB proportion is 4.8%. However, owing to the size proportion of the grain and GB, the phenomenon of ferroelectric disappearance seems unreasonable. Therefore, the "dead layer" interphase assumption has been proved to fall short because of the effect of the GB size at the nanoscale.

Using the FMGB model, the saturation and remanent polarizations remain at almost the same level from P-E loops, and the coercive field decreases, which is consistent with the experimental results.[40–42] As the proportion of GBs decreases, the shielding effect of the GB is weakened, and the domain starts to rotate in grain **2**, as shown in Fig. 6. Figure 6(e) shows that when the applied electric field decreases to $E_1^* = -0.54$, the electric field within grain **2** increases with the proportion of GB decreases, and the internal electric field is more easily affected by the applied electric field, which reduces the difficulty of domain switching; thus, the coercive field decreases, Fig. S6e in
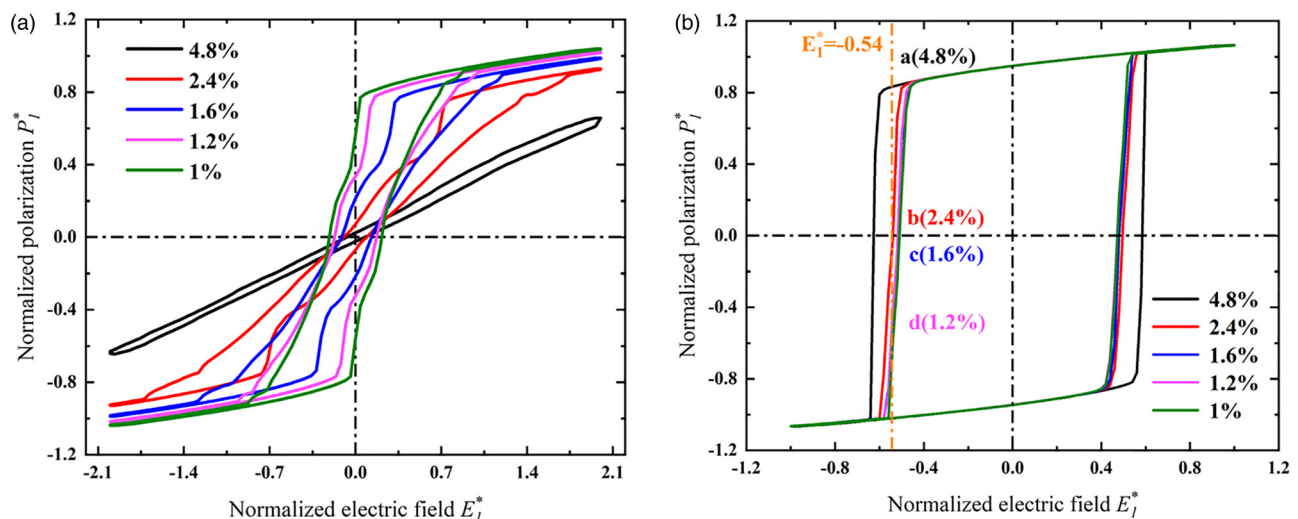

FIG. 5. P-E hysteresis loops with the proportion of GB under different models. (a) "Dead layer" interphase model. (b) FMGB model.
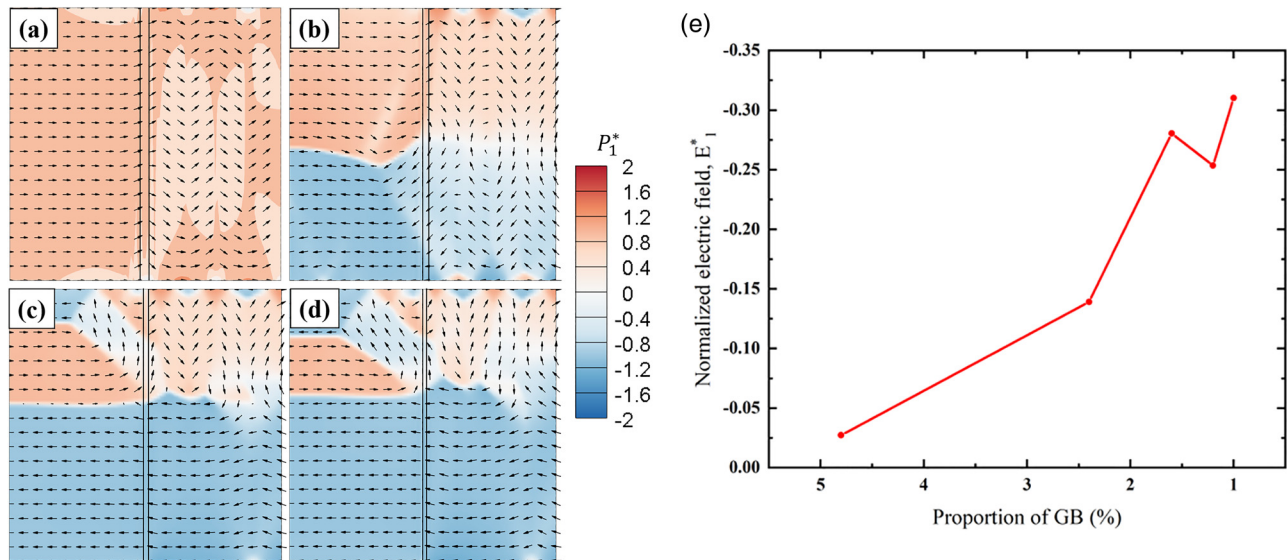
FIG. 6. Domain structures with the electric field, $E^* = E/E_0$ ($E_0 = 96.5\,kV/cm$). (a)–(d) correspond to the four polarization states of different proportions. (a) The proportion of GB is 4.8%. (b) The proportion of GB is 2.4%. (c) The proportion of GB is 1.6%. (d) The proportion of GB is 1.2%. (e) The average normalized electric field E_1^* in grain **2**.

the supplementary material. The distribution of the local electric field shows the nonlinear response near the GB, which is consistent with the experiment.[43] A detailed discussion can be found in the supplementary material.

The FMGB model was used to simulate the domain structures of the bi-crystal in the remanent polarization state, and the results are shown in Fig. 7. As the proportion of GBs decreases, the polarization enhancement phenomenon caused by the interface nearly
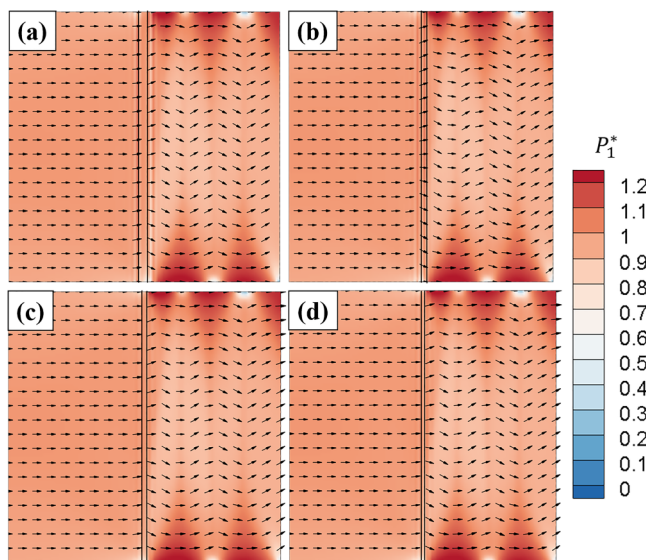

FIG. 7. Under the FMGB model, domain structures at remanent polarization with different proportions of GB. (a) The proportion of GB is set to 4.8%. (b) The proportion of GB is set to 2.4%. (c) The proportion of GB is set to 1.6%. (d) The proportion of GB is set to 1%. The "domain continuity" phenomenon and the polarization enhancement near the interface can be observed significantly.

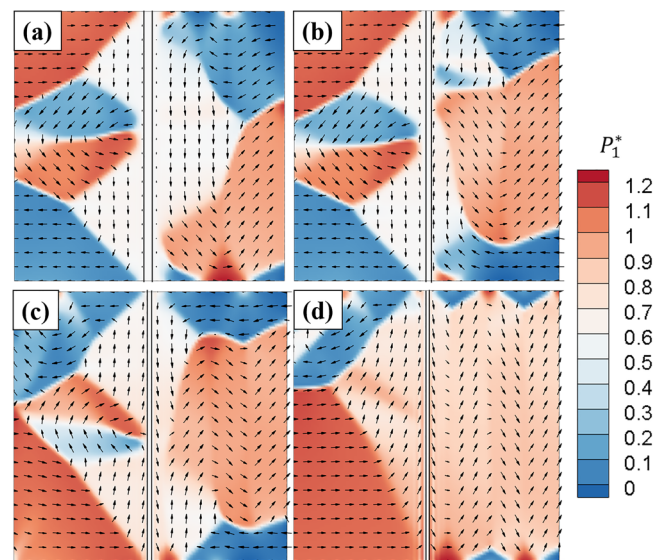**FIG. 8.** Under the "dead layer" model, domain structures at remanent polarization with different proportions of GB. (a) The proportion of GB is set to 4.8%. (b) The proportion of GB is set to 2.4%. (c) The proportion of GB is set to 1.6%. (d) The proportion of GB is set to 1%. Even if the proportion of GB is small, a strong depolarization effect is still observed, but not the "domain continuity" phenomenon.

06 January 2025 07:46:18

disappears. The long-range elastic and electrostatic interaction between grains is enhanced, and the domain continuity phenomenon can still be observed. Domain continuity means the domain structure inside a grain interacts with that of another neighboring grain gradually changing the polarization direction of the GBs, and it is a stationary state in this paper. However, the above phenomena cannot be observed in the "dead layer" model, which is limited by its assumptions, as shown in Fig. 8. By adopting the FMGB model, fatigue resistance and mechanical–electrical coupling performance can be obtained by designing nano-graded polycrystalline ferroelectrics. The electric breakdown resistance and energy storage performance of ferroelectric ceramic capacitors can also be improved predictably by designing the grain arrangement.[44,45]

V. CONCLUSION

Considering the important role of grains in forming GBs, we herein propose a new GB thermodynamic model. This model contains the properties and structural characteristics of the GB and is based on the formation mechanism. From the perspective of energy and electromechanical equations, we present an analytical method for investigating GB properties such as the Curie–Weiss temperature, elasticity, and permittivity coefficient. Those results show that the parameters are related to the orientation difference between adjacent grains and the state of the GB. Previous assumptions about GBs can be derived by simplifying this new model. Integrating the above results into the phase field finite element method, we find some new phenomena that had not been previously reported by similar simulations, such as the shielding effect, polarization enhancement, domain continuity, and spontaneous polarization on the GB. An analysis of the size effect of this new model by changing the proportion of GBs is presented herein; the simulation results show a strong correlation between depolarization, domain continuity, and the proportion of GBs. It should be noted that the FMGB model is a general mesoscopic scale symmetric tilt GB model. Inducing the five independent parameters into the FMGB model will enable it to describe more kinds of GBs. The accurate parameter values of the FMGB model need to be obtained from experiments. Energy density modification like the flexoelectric energy density for the FMGB model will extend its application field, such as the effect of GB migration. The proposed model is conducive to solving the problem of developing a mesoscopic description of GBs and is beneficial to broadening the application of interface engineering.

SUPPLEMENTARY MATERIAL

See the supplementary material for the analyzation of parameters, the domain structure evolution of the previous GB models, and the comparison with experiments.

AUTHOR DECLARATIONS

Conflict of Interest

The authors have no conflicts to disclose.

Author Contributions

Xuhui Lou: Conceptualization (equal); Data curation (equal); Formal analysis (lead); Investigation (lead); Methodology (lead); Software (equal); Validation (equal); Visualization (lead); Writing – original draft (lead); Writing – review & editing (equal). **Xu Hou:** Conceptualization (equal); Data curation (equal); Investigation (equal); Methodology (equal); Software (equal); Writing – review & editing (equal). **Yujun Chen:** Data curation (equal); Formal analysis (equal); Investigation (equal); Writing – review & editing (equal). **Jianxiang Wang:** Data curation (equal); Formal analysis (equal); Validation (equal); Writing – review & editing (equal). **Shengyou Yang:** Data curation (equal); Formal analysis (equal); Validation (equal); Writing – review & editing (equal). **Haidong Fan:** Data curation (equal); Formal analysis (equal); Resources (equal); Validation (equal); Writing – review & editing (equal). **Jie Wang:** Conceptualization (equal); Data curation (equal); Formal analysis (equal); Investigation (supporting); Methodology (supporting); Resources (supporting); Software (supporting); Supervision (supporting); Validation (equal); Visualization (equal); Writing – review & editing (equal). **Xiaobao Tian:** Conceptualization (supporting); Data curation (equal); Formal analysis (equal); Funding acquisition (supporting); Investigation (supporting); Methodology (supporting); Project administration (supporting); Resources (supporting); Software (supporting); Supervision (supporting); Validation (supporting); Visualization (supporting); Writing – review & editing (equal).

DATA AVAILABILITY

The data that support the findings of this study are available within the article and its supplementary material.

REFERENCES

[1]J. F. Scott, "Ferroelectric memories," in *Springer Series in Advanced Microelectronics* (Springer, 2000), Vol. 3, pp. 2–9.

[2]H. Simons, A. King, W. Ludwig, C. Detlefs, W. Pantleon, S. Schmidt, F. Stöhr, I. Snigireva, A. Snigirev, and H. F. Poulsen, "Dark-field X-ray microscopy for multiscale structural characterization," Nat. Commun. **6**, 6098 (2015).

[3]H. Simons, A. B. Haugen, A. C. Jakobsen, S. Schmidt, F. Stöhr, M. Majkut, C. Detlefs, J. E. Daniels, D. Damjanovic, and H. F. Poulsen, "Long-range symmetry breaking in embedded ferroelectrics," Nat. Mater. **17**, 814–819 (2018).

[4]J. Wang, W. Shu, T. Shimada, T. Kitamura, and T. Y. Zhang, "Role of grain orientation distribution in the ferroelectric and ferroelastic domain switching of ferroelectric polycrystals," Acta Mater. **61**, 6037–6049 (2013).

[5]S. B. Lee, W. Sigle, and M. Rühle, "Investigation of grain boundaries in abnormal grain growth structure of TiO_2-excess $BaTiO_3$ by TEM and EELS analysis," Acta Mater. **50**, 2151–2162 (2002).

[6]L. Wang, J. Teng, P. Liu, A. Hirata, E. Ma, Z. Zhang, M. Chen, and X. Han, "Grain rotation mediated by grain boundary dislocations in nanocrystalline platinum," Nat. Commun. **5**, 4402 (2014).

[7]R. C. DeVries and J. E. Burke, "Microstructure of barium titanate ceramics," J. Am. Ceram. Soc. **40**, 200–206 (1957).

06 January 2025 07:46:18

[8]S. Mantri, J. Oddershede, D. Damjanovic, and J. E. Daniels, "Ferroelectric domain continuity over grain boundaries," Acta Mater. **128**, 400–405 (2017).

[9]W. Shu, J. Wang, and T. Y. Zhang, "Effect of grain boundary on the electromechanical response of ferroelectric polycrystals," J. Appl. Phys. **112**, 064108 (2012).

[10]J. Y. Li, R. C. Rogan, E. Üstündag, and K. Bhattacharya, "Domain switching in polycrystalline ferroelectric ceramics," Nat. Mater. **4**, 776–781 (2005).

[11]S. Choudhury, Y. L. Li, C. E. Krill, and L. Q. Chen, "Phase-field simulation of polarization switching and domain evolution in ferroelectric polycrystals," Acta Mater. **53**, 5313–5321 (2005).

[12]S. Choudhury, Y. Li, C. Krill, and L. Q. Chen, "Effect of grain orientation and grain size on ferroelectric domain switching and evolution: Phase field simulations," Acta Mater. **55**, 1415–1426 (2007).

[13]M. H. Frey, Z. Xu, P. Han, and D. A. Payne, "Role of interfaces on an apparent grain size effect on the dielectric properties for ferroelectric barium titanate ceramics," Ferroelectrics **206**, 337–353 (1998).

[14]A. Y. Emelyanov, N. A. Pertsev, S. Hoffmann-Eifert, U. Böttger, and R. Waser, "Grain-boundary effect on the Curie-Weiss law of ferroelectric ceramics and polycrystalline thin films: Calculation by the method of effective medium," J. Electroceram. **9**, 5–16 (2002).

[15]Z. Cai, C. Zhu, L. Wu, B. Luo, P. Feng, and X. Wang, "Vortex domain configuration for energy-storage ferroelectric ceramics design: A phase-field simulation," Appl. Phys. Lett. **119**, 032901 (2021).

[16]A. N. Morozovska, E. A. Eliseev, Y. M. Fomichov, Y. M. Vysochanskii, V. Y. Reshetnyak, and D. R. Evans, "Controlling the domain structure of ferroelectric nanoparticles using tunable shells," Acta Mater. **183**, 36–50 (2020).

[17]T. Shimada, X. Wang, S. Tomoda, P. Marton, C. Elsässer, and T. Kitamura, "Coexistence of rectilinear and vortex polarizations at twist boundaries in ferroelectric PbTiO$_3$ from first principles," Phys. Rev. B **83**, 094121 (2011).

[18]X. Tian, X. He, and J. Lu, "Atomic scale study of the anti-vortex domain structure in polycrystalline ferroelectric," Philos. Mag. **98**, 118–138 (2018).

[19]J. Wang, Y. Yu, J. He, J. Wang, B. Ma, X. Chao, Z. Yang, and D. Wu, "Synergy of valence band modulation and grain boundary engineering leading to improved thermoelectric performance in SnTe," ACS Appl. Energy Mater. **4**, 14608–14617 (2021).

[20]C. Wang, H. Duan, C. Chen, P. Wu, D. Qi, H. Ye, H. Jin, H. L. Xin, and K. Du, "Three-Dimensional atomic structure of grain boundaries resolved by atomic-resolution electron tomography," Matter **3**, 1999–2011 (2020).

[21]C. Zaefferer, J.-C. Kuo, Z. Zhao, M. Winning, D. Raabe, and H. Ye, "On the influence of the grain boundary misorientation on the plastic deformation of aluminum bicrystals," Acta Mater. **51**, 4719–4735 (2003).

[22]D. M. Marincel, H. Zhang, S. Jesse, A. Belianinov, M. B. Okatan, S. V. Kalinin, W. M. Rainforth, I. M. Reaney, C. A. Randall, and S. Trolier-McKinstry, "Domain wall motion across various grain boundaries in ferroelectric thin films," J. Am. Ceram. Soc. **98**, 1848–1857 (2015).

[23]R. A. De Souza, "The formation of equilibrium space-charge zones at grain boundaries in the perovskite oxide SrTiO$_3$," Phys. Chem. Chem. Phys. **11**, 9939–9969 (2009).

[24]W. Rheinheimer, J. P. Parras, J. H. Preusker, R. A. De Souza, and M. J. Hoffmann, "Grain growth in strontium titanate in electric fields: The impact of space-charge on the grain-boundary mobility," J. Am. Ceram. Soc. **102**, 3779–3790 (2019).

[25]C. A. Randall, N. Kim, J. P. Kucera, W. Cao, and T. R. Shrout, "Intrinsic and extrinsic size effects in fine-grained morphotropic-phase-boundary lead zirconate titanate ceramics," J. Am. Ceram. Soc. **81**, 677–688 (1998).

[26]M. J. Hoffmann, M. Hammer, A. Endriss, and D. C. Lupascu, "Correlation between microstructure, strain behavior, and acoustic emission of soft PZT ceramics," Acta Mater. **49**, 1301–1310 (2001).

[27]Z. Zhao, V. Buscaglia, M. Viviani, M. T. Buscaglia, L. Mitoseriu, A. Testino, M. Nygren, M. Johnsson, and P. Nanni, "Grain-size effects on the ferroelectric behavior of dense nanocrystalline BaTiO$_3$ ceramics," Phys. Rev. B **70**, 024107 (2004).

[28]Y. Wang, W. J. Chen, X. Y. Zhang, W. J. Ma, B. Wang, and Y. Zheng, "Highly reliable bipolar resistive switching in sol-gel derived lanthanum-doped PbTiO$_3$ thin film: Coupling with ferroelectricity?," Acta Mech. Sinica **30**, 526–532 (2014).

[29]C. S. Kim, A. D. Rollett, and G. S. Rohrer, "Grain boundary planes: New dimensions in the grain boundary character distribution," Scr. Mater. **54**, 1005–1009 (2006).

[30]S. B. Lee, J.-H. Lee, Y.-H. Cho, D.-Y. Kim, W. Sigle, F. Phillipp, and P. A. van Aken, "Grain-boundary plane orientation dependence of electrical barriers at Σ5 boundaries in SrTiO$_3$," Acta Mater. **56**, 4993–4997 (2008).

[31]W. T. Read and W. Shockley, "Dislocation models of crystal grain boundaries," Phys. Rev. **78**, 275–289 (1950).

[32]A. Vondrous, M. Reichardt, and B. Nestler, "Growth rate distributions for regular two-dimensional grains with Read-Shockley grain boundary energy," Modelling Simul. Mater. Sci. Eng. **22**, 025014 (2014).

[33]D. Liu, J. Wang, H. M. Jafri, X. Wang, X. Shi, D. Liang, C. Yang, X. Cheng, and H. Huang, "Phase-field simulations of vortex chirality manipulation in ferroelectric thin films," npj Quantum Mater. **7**, 34 (2022).

[34]F. Li, S. Zhang, Z. Xu, and L.-Q. Chen, "The contributions of polar nanoregions to the dielectric and piezoelectric responses in domain-engineered relaxor-PbTiO$_3$ crystals," Adv. Funct. Mater. **27**, 1700310 (2017).

[35]H. Duan, J. Wang, and Z. Huang, "Micromechanics of composites with interface effects," Acta Mech. Sinica **38**, 222025 (2022).

[36]Y. A. Genenko, J. Glaum, O. Hirsch, H. Kungl, M. J. Hoffmann, and T. Granzow, "Aging of poled ferroelectric ceramics due to relaxation of random depolarization fields by space-charge accumulation near grain boundaries," Phys. Rev. B **80**, 024109 (2009).

[37]S. Gorfman, H. Simons, T. Iamsasri, S. Prasertpalichat, D. P. Cann, H. Choe, U. Pietsch, Y. Watier, and J. L. Jones, "Simultaneous resonant x-ray diffraction measurement of polarization inversion and lattice strain in polycrystalline ferroelectrics," Sci. Rep. **6**, 20829 (2016).

[38]J. Glaum, H. Simons, M. Acosta, and M. Hoffman, "Tailoring the piezoelectric and relaxor properties of (Bi$_{1/2}$Na$_{1/2}$)TiO$_3$-BaTiO$_3$ via zirconium doping," J. Am. Ceram. Soc. **96**, 2881–2886 (2013).

[39]Y. Zhang, B. Liu, and D. Fang, "Stress-induced phase transition and deformation behavior of BaTiO$_3$," J. Appl. Phys. **110**, 054109 (2011).

[40]B. M. Jin, J. Kim, and S. C. Kim, "Effects of grain size on the electrical properties of PbZr$_{0.52}$Ti$_{0.48}$O$_3$ ceramics," Appl. Phys. A: Mater. Sci. Process. **65**, 53–56 (1997).

[41]T. Takeuchi, M. Tabuchi, I. Kondoh, N. Tamari, and H. Kageyama, "Synthesis of dense lead titanate ceramics with submicrometer grains by spark plasma sintering," J. Am. Ceram. Soc. **83**, 541–544 (2000).

[42]J. S. Liu, S. R. Zhang, H. Z. Zeng, C. T. Yang, and Y. Yuan, "Coercive field dependence of the grain size of ferroelectric films," Phys. Rev. B **72**, 172101 (2005).

[43]D. M. Marincel, H. R. Zhang, J. Britson, A. Belianinov, S. Jesse, S. V. Kalinin, L. Q. Chen, W. M. Rainforth, I. M. Reaney, C. A. Randall, and S. Trolier-McKinstry, "Domain pinning near a single-grain boundary in tetragonal and rhombohedral lead zirconate titanate films," Phys. Rev. B **91**, 134113 (2015).

[44]S. Hyun, H. Park, Y. Kim, M. Park, Y. Lee, H. Kim, Y. Kwon, T. Moon, K. Kim, Y. Lee, B. Kim, and C. Hwang, "Dispersion in ferroelectric switching performance of polycrystalline Hf$_{0.5}$Zr$_{0.5}$O$_2$ thin films.," ACS. Appl. Mater. Inter. **10**, 35374–35384 (2018).

[45]M. Yang, Z. Luo, Z. Mi, J. Zhao, E. S. Pei, and M. Alexe, "Piezoelectric and pyroelectric effects induced by interface polar symmetry," Nature **584**, 377–381 (2020).